

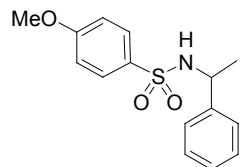
SUPPORTING INFORMATION

Imido Transfer from Bis(imido)ruthenium(VI) Porphyrins to Hydrocarbons: Effect of Imido Substituents, C–H Bond Dissociation Energies, and Ru^{VI/V} Reduction Potentials

Sarana Ka-Yan Leung, Wai-Man Tsui, Jie-Sheng Huang,* Chi-Ming Che,* Jiang-Lin Liang, and Nianyong Zhu

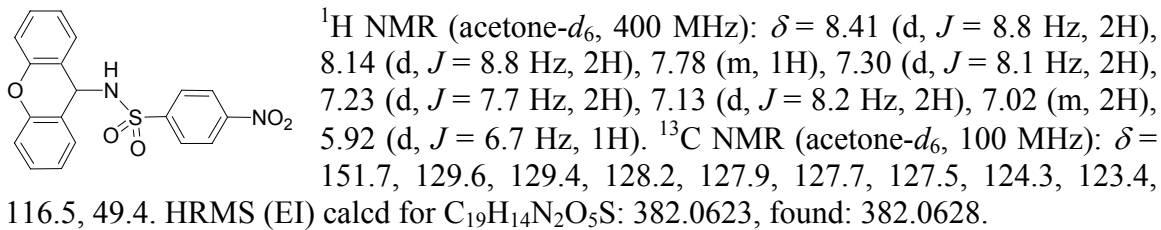
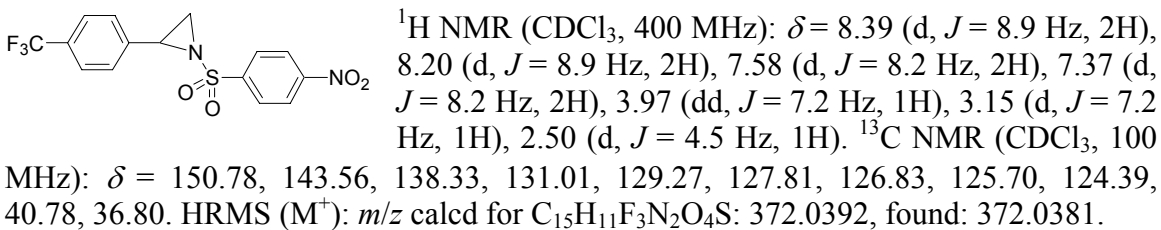
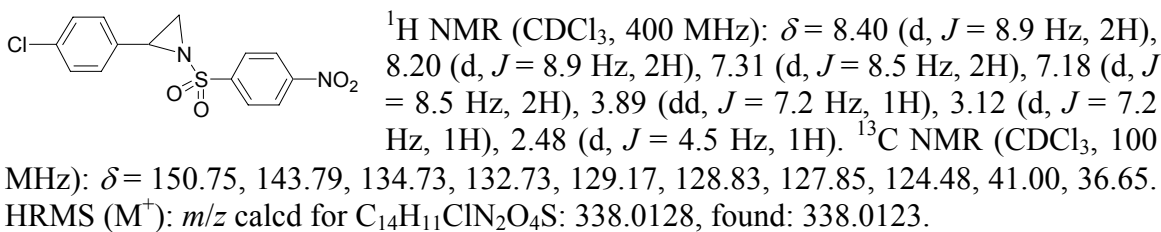
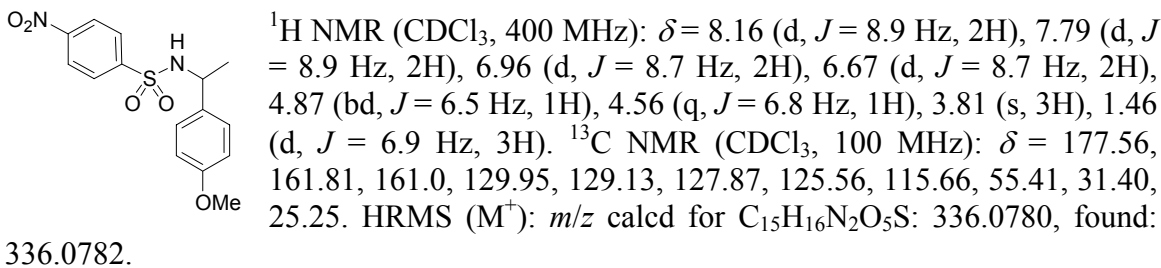
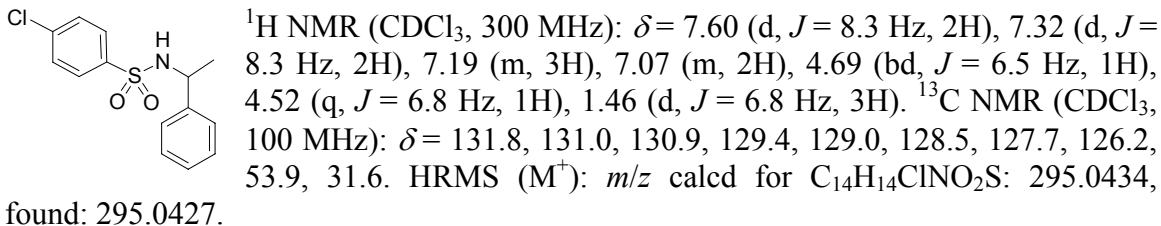
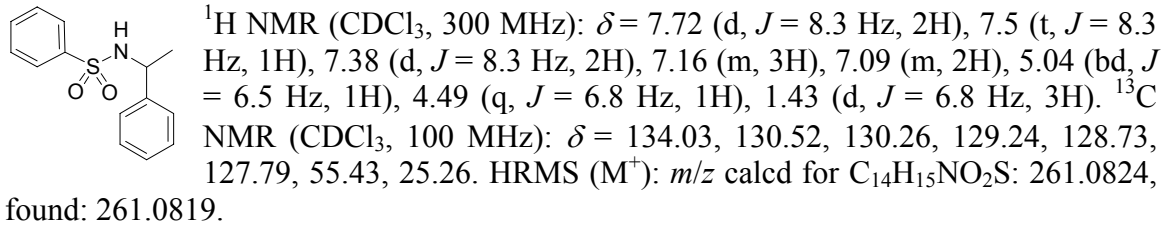
General. Ethylbenzene-*d*₁₀ (Aldrich) was used as received. Pyrazole was recrystallized from petroleum ether. Dihydroanthracene, fluorene, and xanthene were recrystallized from EtOH. *p*-Nitrostyrene, indene, *p*-nitroethylbenzene, and toluene were purified by passing through a column of activated alumina. Other hydrocarbons and CH₂Cl₂ were purified as described previously.¹ The purity of all the hydrocarbons was checked by GC or ¹H NMR analysis. PhI=NSO₂R (SO₂R = Ms, Ts, Bs, Cs, Ns),^{2,3} [Ru^{II}(Por)(CO)] (Por = TPP,⁴ TMP,⁵ 2,6-Cl₂TPP,⁶ F₂₀-TPP⁷), and [Ru^{VI}(TPP)(NTs)₂]¹ were prepared by literature methods. UV-vis spectra were recorded on a Hewlett-Packard 8453 diode array spectrophotometer interfaced with IBM compatible PC or a Perkin-Elmer Lambda 19 spectrophotometer. ¹H NMR spectra were measured on Brucker DPX 300 and 400 spectrometers. Chemical shifts (δ ppm) are relative to tetramethylsilane. IR spectra were obtained on a Bio-Rad FT-IR spectrometer. FAB mass spectra were recorded on a Finnigan MAT 95 mass spectrometer using 3-nitrobenzyl alcohol as matrix. Electrospray mass spectra (ESMS) were measured on a Finnigan LCQ quadrupole ion trap mass spectrometer (samples were dissolved in HPLC CH₂Cl₂). Cyclic voltammograms were recorded on a Princeton Applied Research Model 273A potentiostat/galvanostat coulometer and Model 270/250 universal programmer using a three-electrode cell system (working electrode: glassy carbon, counter electrode: platinum wire, reference electrode: 0.1 M Ag/AgNO₃ in MeCN). The electrolyte, [NBuⁿ₄]PF₆ (Avocado), was recrystallized three times from hot EtOH and dried in vacuo at 80 °C for 12 h before use. Ferrocene was used as an internal standard. Elemental analyses were performed by Institute of Chemistry, the Chinese Academy of Sciences.

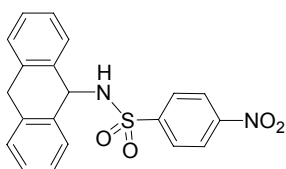
Characterization of Aziridination/Amidation Products.



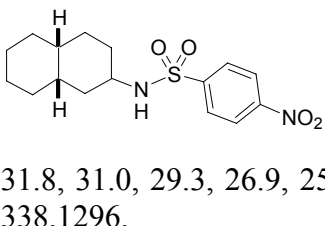
found: 291.0931.

¹H NMR (CDCl₃, 300 MHz): δ = 7.65 (d, *J* = 8.3 Hz, 2H), 7.18 (m, 5H), 7.00 (m, 2H), 4.61 (bd, *J* = 6.5 Hz, 1H), 4.46 (q, *J* = 6.8 Hz, 1H), 3.28 (s, 3H), 1.44 (d, *J* = 6.8 Hz, 3H). ¹³C NMR (CDCl₃, 100 MHz): δ = 126.0, 125.4, 124.4, 123.0, 111.5, 111.4, 111.1, 110.8, 52.4, 50.4, 26.5. HRMS (M⁺): *m/z* calcd for C₁₅H₁₇NO₃S: 291.0929,





¹H NMR (CDCl₃, 400 MHz): δ = 8.14 (d, *J* = 8.7 Hz, 2H), 7.73 (d, *J* = 8.7 Hz, 2H), 7.36 (d, *J* = 7.1 Hz, 2H), 7.18 (m, 6H), 5.65 (d, *J* = 5.1 Hz, 1H), 4.95 (d, *J* = 5.1 Hz, 1H), 3.91 (d, *J* = 18.2 Hz, 1H), 3.79 (d, *J* = 18.2 Hz, 1H). ¹³C NMR (CDCl₃, 100 MHz): δ = 149.9, 147.1, 137.6, 135.2, 128.9, 128.6, 128.3, 128.2, 127.0, 124.2, 57.6, 35.4. HRMS (EI) calcd for C₂₀H₁₆N₂O₄S: 380.0831, found: 380.0826.



¹H NMR (CDCl₃, 400 MHz) (major product): δ = 8.36 (d, *J* = 8.8 Hz, 2H), 8.06 (d, 2H), 4.55 (d, *J* = 7.8 Hz, 1H), 3.20 (m, 1H), 1.76 (m, 2H), 1.71–1.32 (m, 14H). ¹³C NMR (CDCl₃, 75 MHz): δ = 147.9, 128.5, 124.7, 124.6, 54.7, 35.5, 34.7, 34.2, 31.8, 31.0, 29.3, 26.9, 25.8, 21.1. HRMS (EI) calcd for C₁₆H₂₂N₂O₄S: 338.1300, found: 338.1296.

For characterization of the other aziridination/amidation products, see refs 1, 3a, 8–11.

References

- (1) Au, S.-M.; Huang, J.-S.; Yu, W.-Y.; Fung, W.-H.; Che, C.-M. *J. Am. Chem. Soc.* **1999**, *121*, 9120.
- (2) Müller, P.; Baud, C.; Jacquier, Y. *Can. J. Chem.* **1998**, *76*, 738.
- (3) (a) Södergren, M. J.; Alonso, D. A.; Andersson, P. G. *Tetrahedron: Asymmetry* **1997**, *8*, 3563. (b) Södergren, M. J.; Alonso, D. A.; Bedekar, A. V.; Andersson, P. G. *Tetrahedron Lett.* **1997**, *38*, 6897.
- (4) Rillema, D. P.; Nagle, J. K.; Barringer, L. F., Jr.; Meyer, T. J. *J. Am. Chem. Soc.* **1981**, *103*, 56.
- (5) Groves, J. T.; Quinn, R. *Inorg. Chem.* **1984**, *23*, 3844.
- (6) Leung, W.-H.; Che, C.-M.; Yeung, C.-H.; Poon, C.-K. *Polyhedron*, **1993**, *12*, 2331.
- (7) Groves, J. T.; Bonchio, M.; Carofiglio, T.; Shalyaew, K. *J. Am. Chem. Soc.* **1996**, *118*, 8961.
- (8) Mahy, J.-P.; Bedi, G.; Battioni, P.; Mansuy, D. *J. Chem. Soc., Perkin Trans. 2* **1988**, 1517.
- (9) Evans, D. A.; Fad, M. M.; Bilodeau, M. T. *J. Am. Chem. Soc.* **1994**, *116*, 2742.
- (10) Nägeli, I.; Baud, C.; Bernardinelli, G.; Jacquier, Y.; Moran, M.; Müller, P. *Helv. Chim. Acta* **1997**, *80*, 1087.
- (11) Yu, X.-Q.; Huang, J.-S.; Zhou, X.-G.; Che, C.-M. *Org. Lett.* **2000**, *2*, 2233.

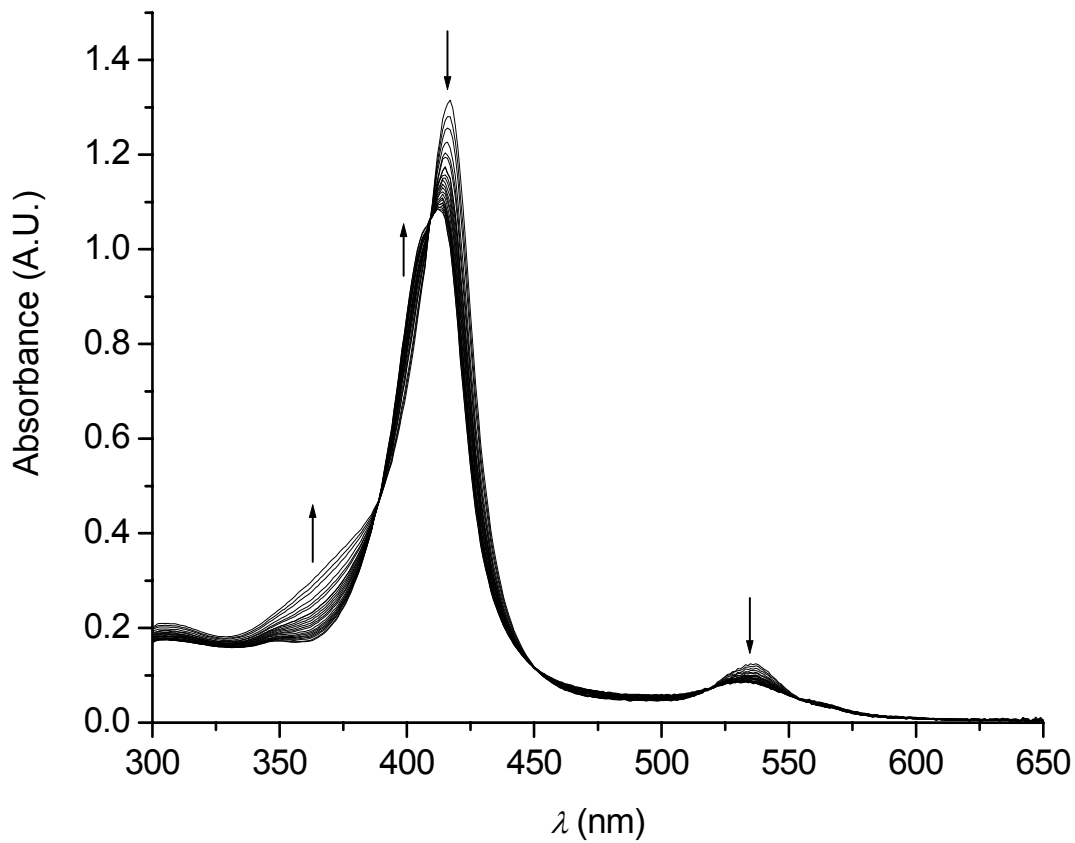


Figure S1. UV-vis spectral changes for reaction of $[\text{Ru}^{\text{VII}}(\text{TMP})(\text{NNs})_2]$ with styrene in CH_2Cl_2 containing pyrazole (2% w/w) at 298 K.

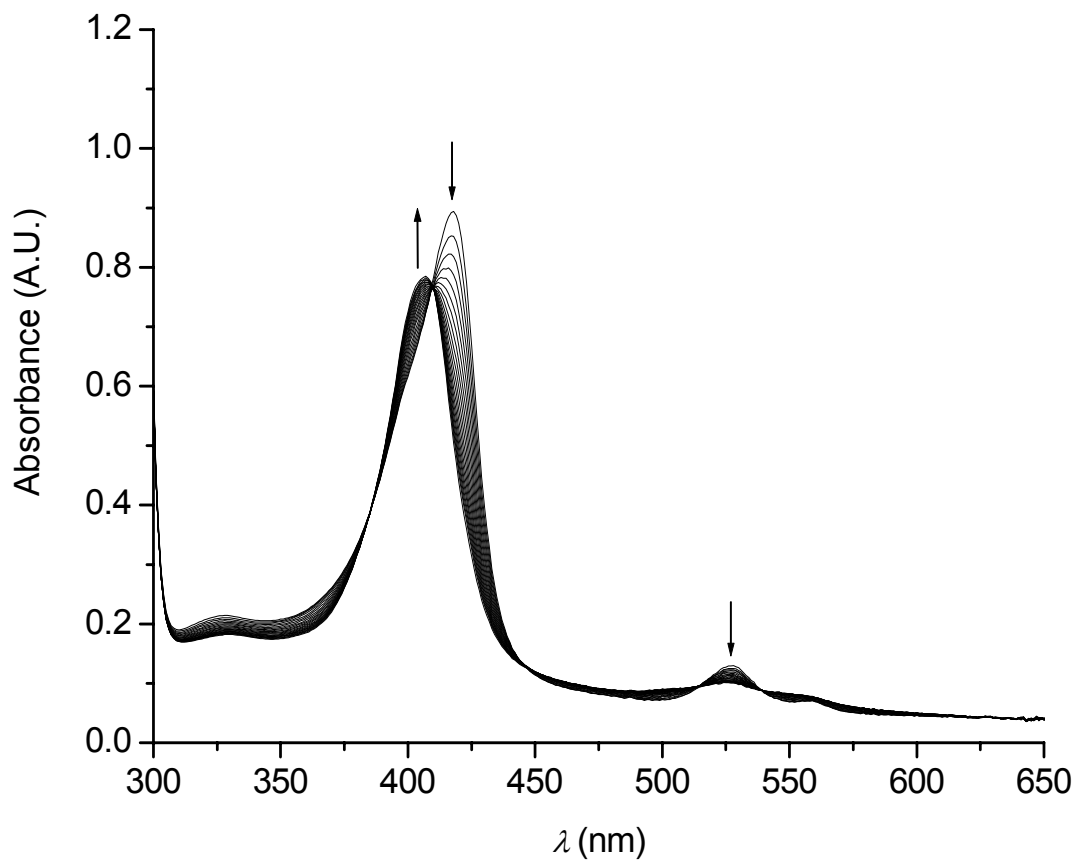


Figure S2. UV-vis spectral changes for reaction of $[\text{Ru}^{\text{VI}}(\text{F}_{20}\text{-TPP})(\text{NTs})_2]$ with styrene in CH_2Cl_2 containing pyrazole (2% w/w) at 298 K.

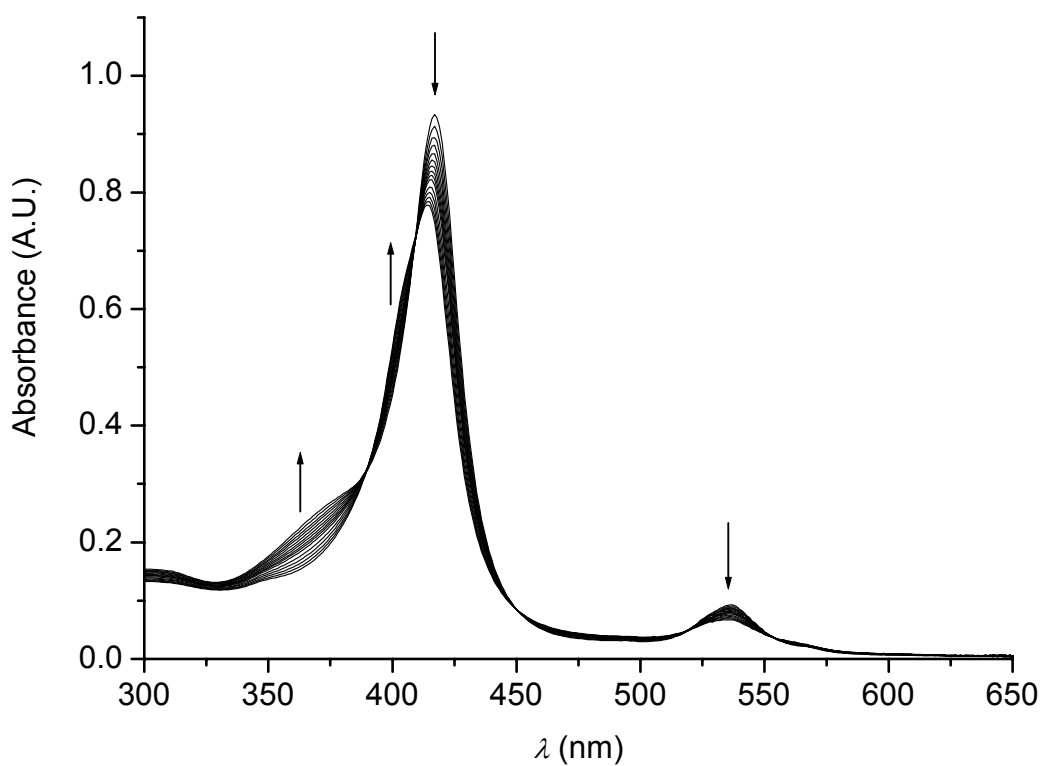


Figure S3. UV-vis spectral changes for reaction of $[\text{Ru}^{\text{VII}}(\text{TMP})(\text{NNs})_2]$ with cumene in CH_2Cl_2 containing pyrazole (2% w/w) at 298 K.

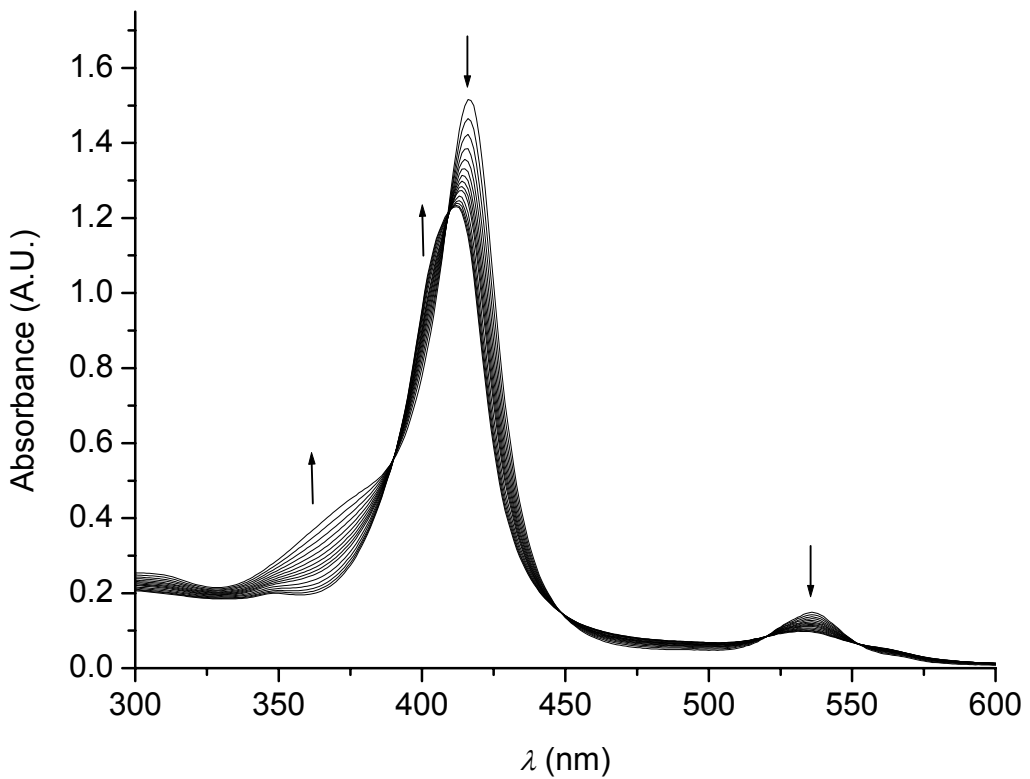


Figure S4. UV-vis spectral changes for reaction of $[\text{Ru}^{\text{VI}}(\text{TMP})(\text{NNs})_2]$ with tetrahydrofuran in CH_2Cl_2 containing pyrazole (2% w/w) at 298 K.

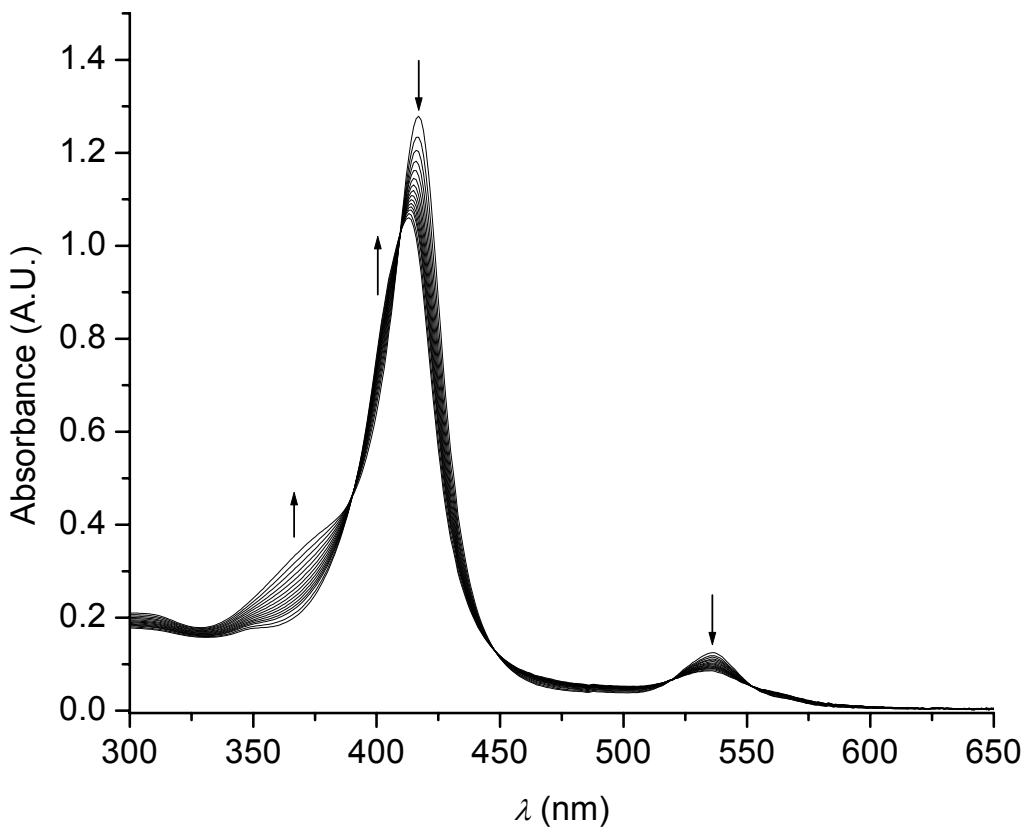


Figure S5. UV-vis spectral changes for reaction of $[\text{Ru}^{\text{VI}}(\text{TMP})(\text{NNs})_2]$ with toluene in CH_2Cl_2 containing pyrazole (2% w/w) at 298 K.

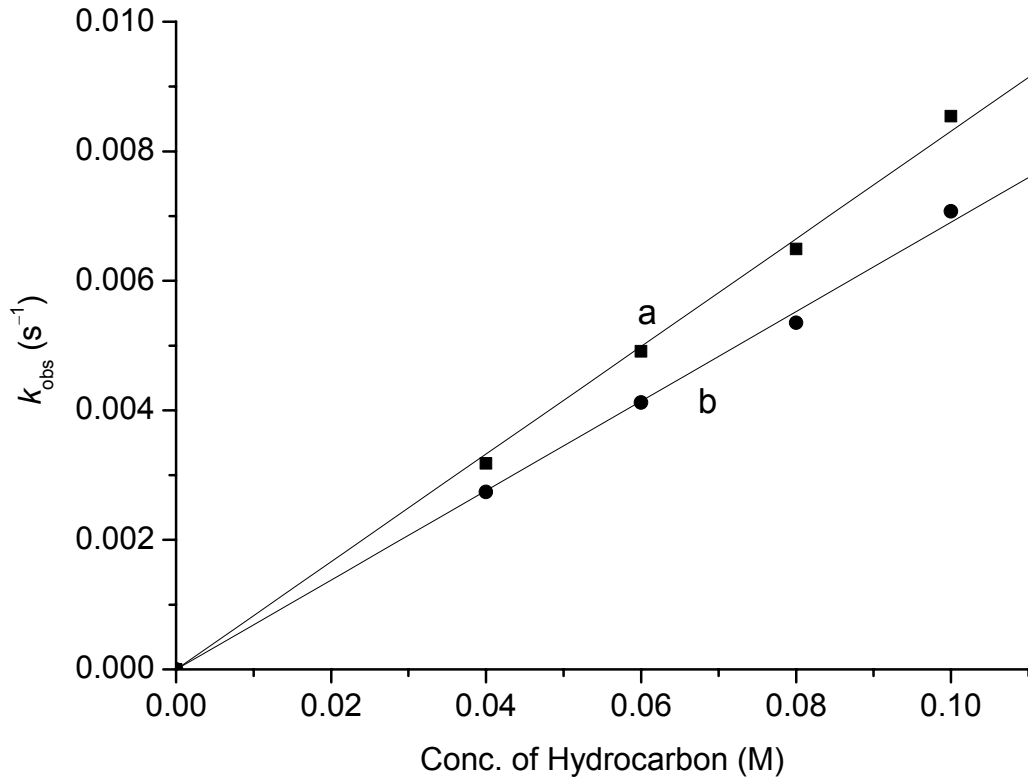


Figure S6. Plots of k_{obs} vs [hydrocarbon] for reaction of $[\text{Ru}^{\text{VI}}(\text{TMP})(\text{NNs})_2]$ with (a) styrene and (b) *p*-chlorostyrene in CH_2Cl_2 containing pyrazole (2% w/w) at 298 K.

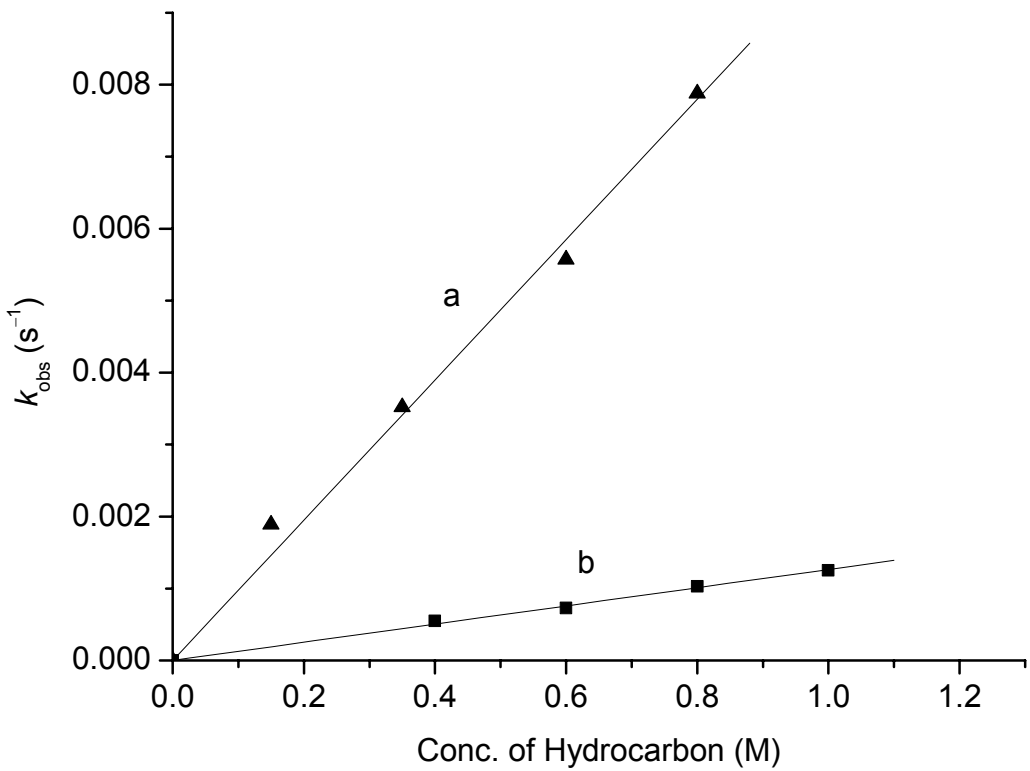


Figure S7. Plots of k_{obs} vs [hydrocarbon] for reaction of $[\text{Ru}^{\text{VI}}(\text{TMP})(\text{NNs})_2]$ with (a) *p*-trifluorostyrene and (b) norbornene in CH_2Cl_2 containing pyrazole (2% w/w) at 298 K.

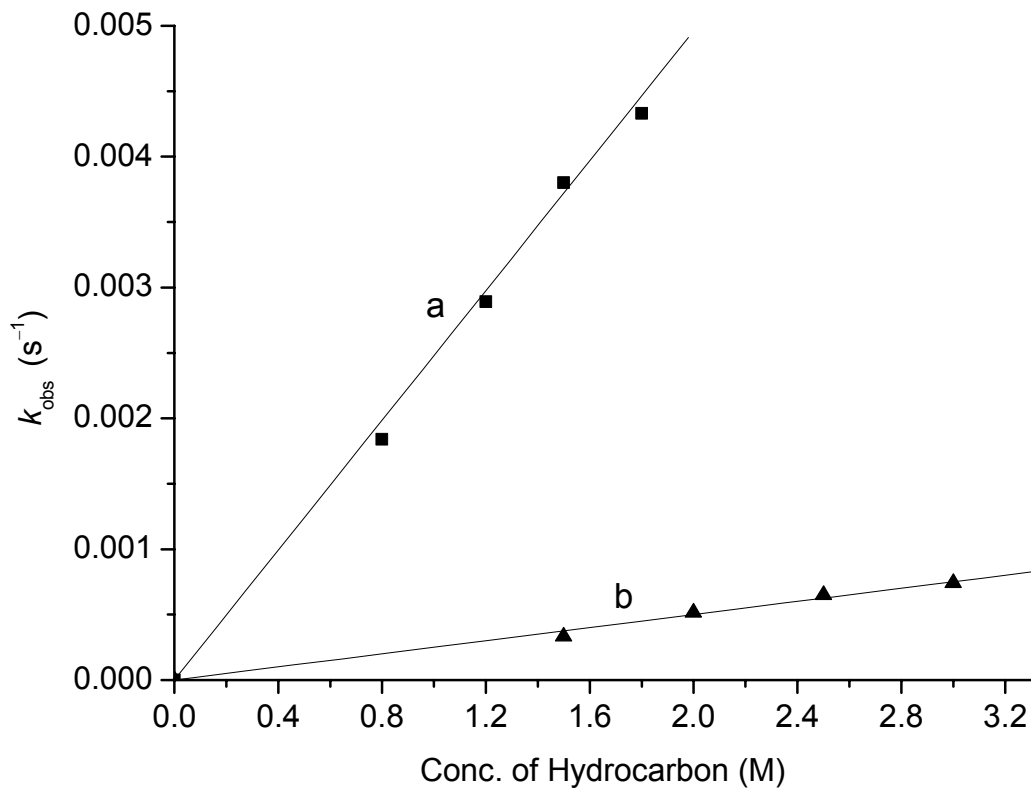


Figure S8. Plots of k_{obs} vs [hydrocarbon] for reaction of $[\text{Ru}^{\text{VI}}(\text{TMP})(\text{NNs})_2]$ with (a) ethylbenzene and (b) cumene in CH_2Cl_2 containing pyrazole (2% w/w) at 298 K.

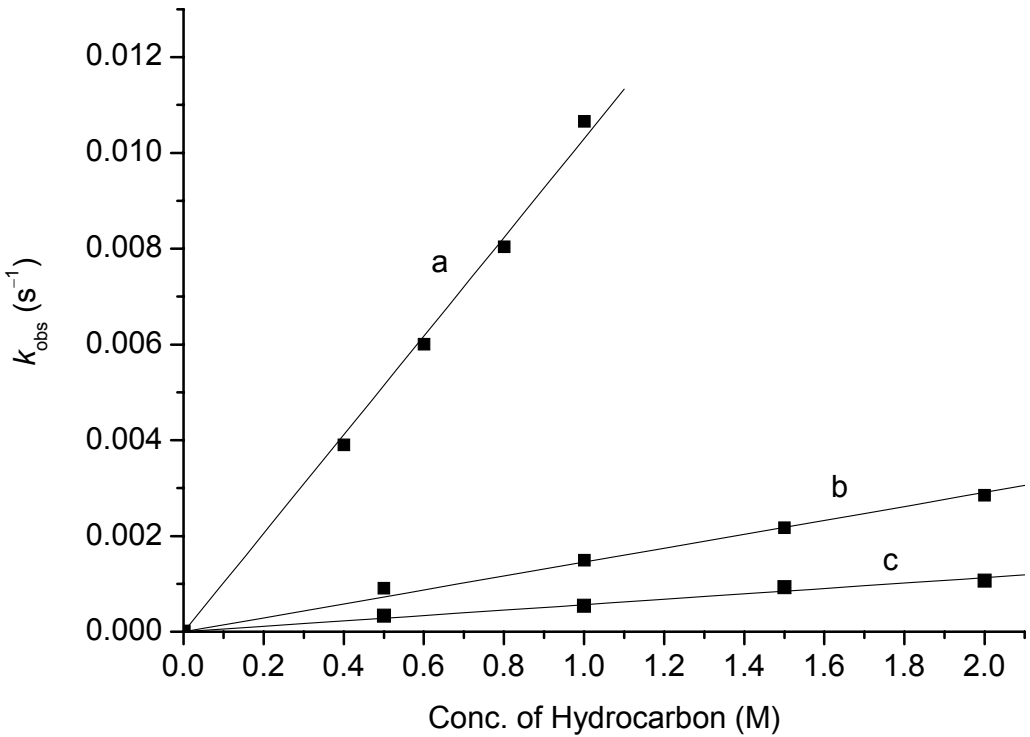


Figure S9. Plots of k_{obs} vs [hydrocarbon] for reaction of (a) $[\text{Ru}^{\text{VI}}(\text{TMP})(\text{NNs})_2]$, (b) $[\text{Ru}^{\text{VI}}(\text{TMP})(\text{NBS})_2]$, and (c) $[\text{Ru}^{\text{VI}}(\text{TMP})(\text{NMs})_2]$ with tetrahydrofuran in CH_2Cl_2 containing pyrazole (2% w/w) at 298 K.

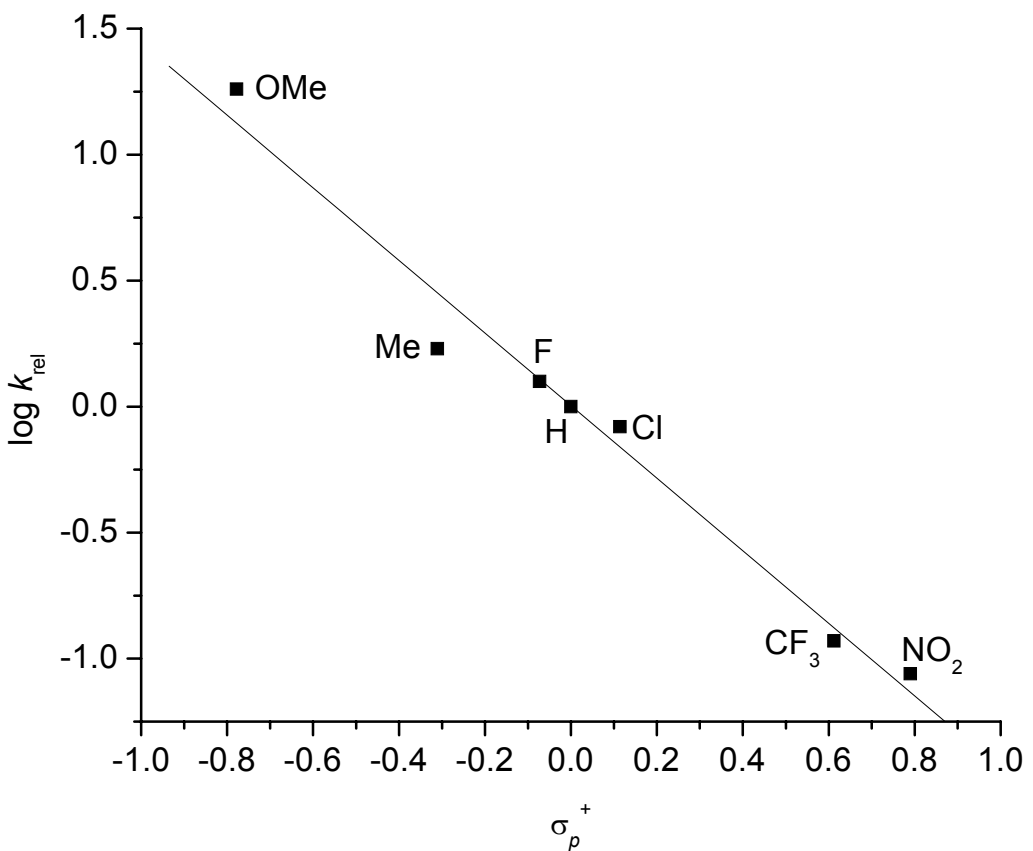


Figure S10. Plot of $\log k_{\text{rel}}$ vs σ_p^+ for reaction of $[\text{Ru}^{\text{VI}}(\text{TMP})(\text{NNs})_2]$ with $p\text{-XC}_6\text{H}_4\text{CH=CH}_2$ ($X = \text{OMe}, \text{Me}, \text{H}, \text{F}, \text{Cl}, \text{CF}_3, \text{NO}_2$) in CH_2Cl_2 containing pyrazole (2% w/w) at 298 K.

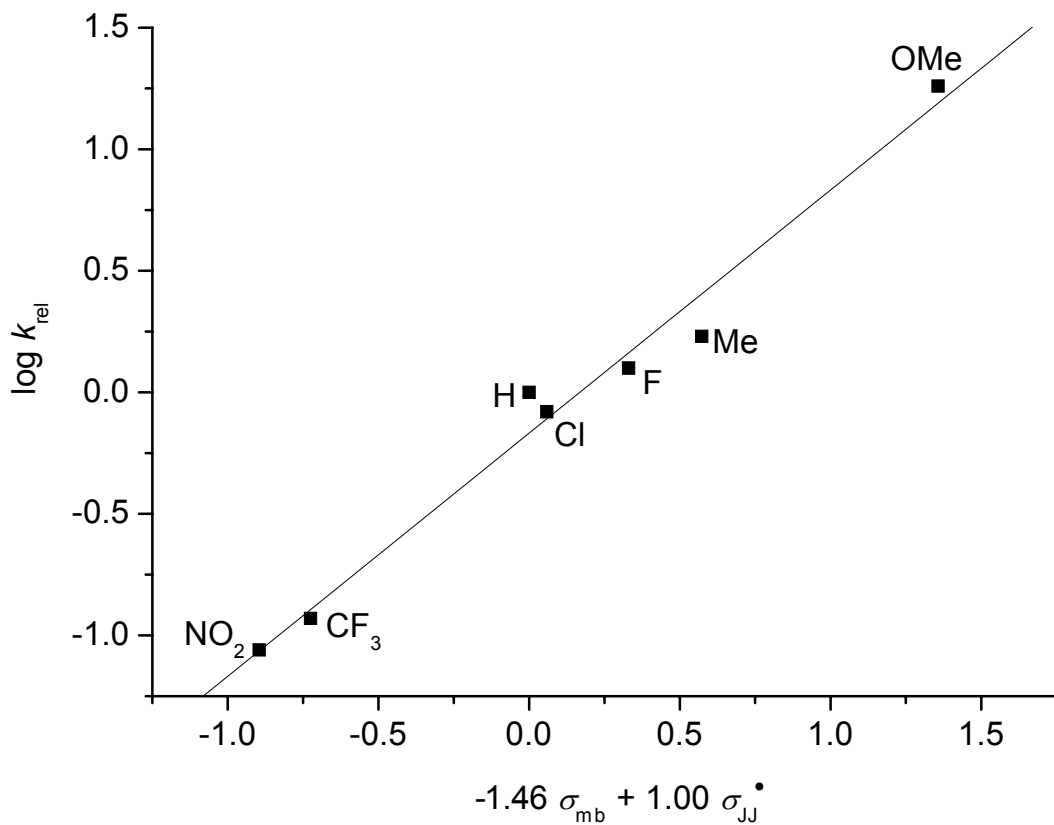


Figure S11. Plot of $\log k_{\text{rel}}$ vs $(\sigma_{\text{mb}}, \sigma_{\text{JJ}^*})$ for reaction of $[\text{Ru}^{\text{VI}}(\text{TMP})(\text{NNs})_2]$ with $p\text{-XC}_6\text{H}_4\text{CH=CH}_2$ ($X = \text{OMe}, \text{Me}, \text{H}, \text{F}, \text{Cl}, \text{CF}_3, \text{NO}_2$) in CH_2Cl_2 containing pyrazole (2% w/w) at 298 K.

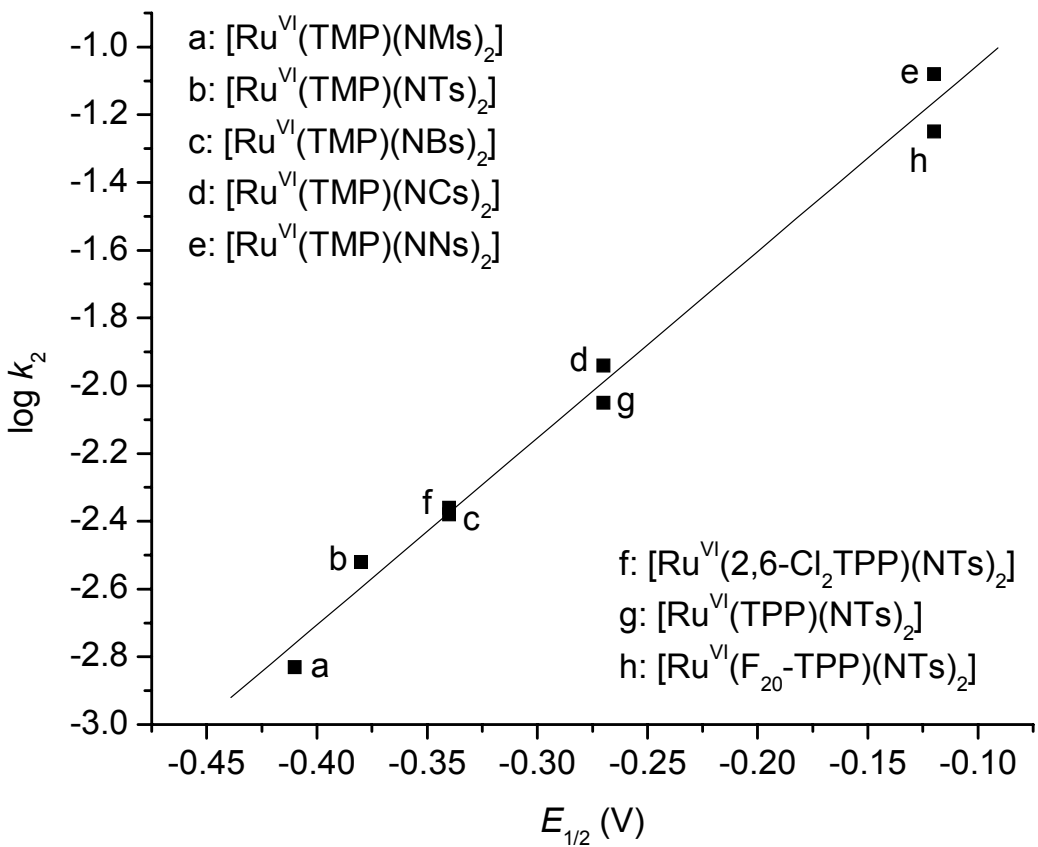


Figure S12. Plot of $\log k_2$ vs $E_{1/2}(\text{Ru}^{\text{VI}/\text{V}})$ for reaction of $[\text{Ru}^{\text{VI}}(\text{Por})(\text{NSO}_2\text{R})_2]$ with styrene in CH_2Cl_2 containing pyrazole (2% w/w) at 298 K.